Gravity-driven migration of bubbles and/or solid particles near a free surface

Marine Guémas, Antoine Sellier, Franck Pigeonneau

Gravity-driven migration of bubbles and/or solid particles near a free surface

M. Guémas[1],[2], A. Sellier[1] and F. Pigeonneau[2]
[1]LadHyx. Ecole polytechnique, 91128 Palaiseau Cédex, France
[2]Surface du Verre et Interfaces, UMR125 CNRS St Gobain, 39 quai Lucien Lefranc, BP 135, 93303 Aubervilliers, Cedex, France
e-mail: marine.guemas@ladhyx.polytechnique.fr
e-mail: sellier@ladhyx.polytechnique.fr

Keywords: Bubble, free surface, surface tension, Stokes flow, Boundary-integral equation, film drainage.

Abstract

We investigate the challenging problem of bubble(s) and rigid particle(s) interacting near a free surface. The time-dependent bubble(s) and free surface shapes are determined for a large range of Bond number by solving the creeping flow induced by the bubble(s) and the particle(s) motion. This works extends the boundary-integral formulation handled in a recent work solely dealing with bubble(s) ascending toward a free surface.

1. Introduction

The gravity-driven motion of bubble(s) interacting with solid particle(s) in a viscous liquid in presence of a free surface is of high interest in applications such as geophysics, chemistry, glass process, ... This task is quite involved due to the interactions occurring between the different solid and evolving surfaces. The *axisymmetric* gravity-driven migration of bubble(s) ascending toward a free surface has been numerically investigated either for bubble with equal surface tension in [4] or unequal surface tension in [1]. In contrast, this work considers, still for axisymmetric geometry, the more-involved case of cluster made of both bubble(s) and solid particle(s). This problem is solved adopting regularized and carefully-selected boundary-integral equations enforced on the entire liquid domain.

2. Challenging time-dependent problem

2.1 Assumptions and relevant axisymmetric quasi-steady Stokes flow

We consider a cluster made of $M \geq 0$ bubbles B_m and/or $N \geq 0$ solid particles $\mathcal{P}_n$ with $M+N \geq 1$ immersed in a Newtonian fluid with uniform density ρ and viscosity μ. This liquid is bounded by a free surface and both the cluster and the liquid are subject to the uniform gravity $\mathbf{g} = -g\mathbf{e}_3$ (with $g > 0$). The bubble B_m, the solid particle $\mathcal{P}_n$ and the free surface have smooth and time-dependent surfaces $S_m(t)$ with uniform surface tension γ_n, $\Sigma_n(t)$ and $S_0(t)$ with uniform surface tension γ_0, respectively.

As illustrated in Figure 1 for $M = N = 1$, all surfaces $S_0(t)$, $S_m(t)$ and /or $\Sigma_n(t)$ admit unit normal vector $\mathbf{n}$ directed into the liquid domain $\mathcal{D}(t)$ and *the same* axis of revolution $(O, \mathbf{e}_3)$ (axisymmetric problem).

As the cluster migrates under the gravity, the shapes of the bubble(s) and free surface evolve in time. At initial time, each bubble is spherical with typical radius a and the free surface is the $z = 0$ plane. At any time t, the pressure p_0 above the disturbed free surface $S_0(t)$ and p_m inside the disturbed bubble B_m are assumed to be constant. Each solid particle $\mathcal{P}_n$ with uniform density ρ_n has, for symmetry reasons, time-dependent velocity $U^{(n)}(t)\mathbf{e}_3$. In addition, the liquid flow has pressure $p + \rho\mathbf{g}.\mathbf{x}$ (here $\mathbf{x} = OM$ with O denoting the origin of our Cartesian coordinates) velocity $\mathbf{u}$ and stress tensor $\boldsymbol{\sigma}$. We denote by a the bubble(s) and solid particles typical length scale and by V the typical magnitude of velocities $\mathbf{u}$ and $U^{(n)}(t)$. Assuming that $\mathrm{Re} = \rho V a/\mu \ll 1$, inertial effects are negligible

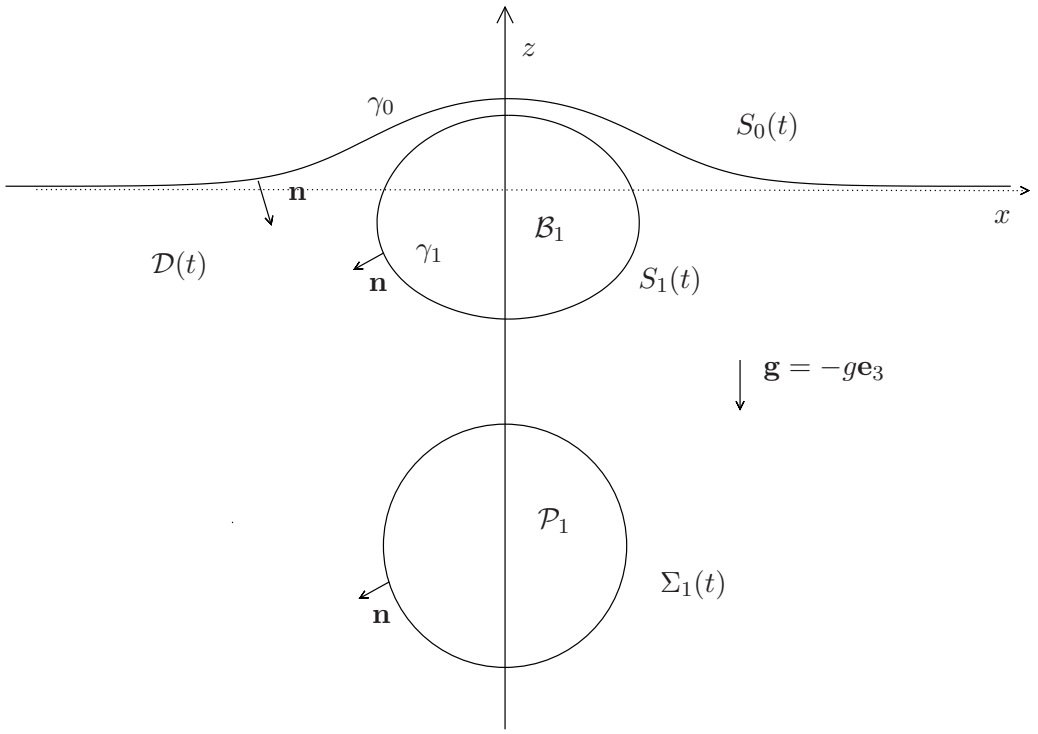

Figure 1: One bubble B_1 and a solid sphere $\mathcal{P}_1$ moving near a free surface $S_0(t)$.

and the flow $(\mathbf{u}, p)$ obeys the following quasi-steady creeping flow equations and boundary conditions

$$\boldsymbol{\nabla} \cdot \mathbf{u} = 0 \text{ and } \mu \boldsymbol{\nabla}^2 \mathbf{u} = \mathbf{grad} p \text{ in } \mathcal{D}(t), \ (\mathbf{u}, p) \to (\mathbf{0}, 0) \text{ as } |\mathbf{x}| \to \infty, \tag{1}$$

$$\boldsymbol{\sigma} \cdot \mathbf{n} = (\rho \mathbf{g} \cdot \mathbf{x} - p_m + \gamma_m \boldsymbol{\nabla}_S \cdot \mathbf{n})\, \mathbf{n} \text{ on } S_m(t) \text{ for } m = 0, ..., M, \tag{2}$$

$$\mathbf{u} = U^{(n)}(t)\mathbf{e}_3 \text{ on } \Sigma_n(t) \text{ for } n = 1, ..., N \tag{3}$$

where $H = [\boldsymbol{\nabla}_S \cdot \mathbf{n}]/2$ is the local average curvature. Assuming bubbles with constant volume, one supplements (1)-(3) with the relations [1]

$$\int_{S_m(t)} \mathbf{u} \cdot \mathbf{n}\, dS = 0 \text{ on } S_m \text{ for m=0,...,M.} \tag{4}$$

For $N \geq 1$ the velocities $U^{(n)}(t)$ are unknown. By symmetry, each solid particle $\mathcal{P}_n$ is torque-free. In addition, each $\mathcal{P}_n$ with negligeable inertia is force-free. This latter property results in the additionnal conditions

$$\int_{\Sigma_n(t)} \mathbf{e}_3 \cdot \boldsymbol{\sigma} \cdot \mathbf{n} dS = (\rho_n - \rho)\mathcal{V}_n\, g \quad \text{for } n = 1, ..., N \tag{5}$$

where ρ_n and $\mathcal{V}_n$ designate the uniform density and volume of the particle $\mathcal{P}_n$.

The material surface(s) $S_m(t)$ have velocity $\mathbf{V}$. Since there is no mass transfer across the surfaces $S_m(t)$, one has

$$\mathbf{V} \cdot \mathbf{n} = \mathbf{u} \cdot \mathbf{n} \text{ on } S_m \text{ for } m = 0, ..., M. \tag{6}$$

2.2 Proposed tracking algorithm for the time-dependent entire liquid boundary

We compute the time-dependent shape of the free surface, the bubble(s) and particle(s) surface(s) by running at each time t the following steps :

[1] Note that (4) indeed also holds for $m = 0$ because $\mathbf{u}$ is divergence-free and $\mathbf{u} \to \mathbf{0}$.

Step 1: From the knowledge at time t of the liquid domain $\mathcal{D}(t)$, one first computes the quantity $\boldsymbol{\nabla}_S \cdot \mathbf{n}$ on each surface $S_m(t)$.

Step 2: One then solves at time t the relations (1)-(5) to get the unknown velocities $U^{(n)}(t)$ and the fluid velocity $\mathbf{u}$ on each surface $S_m(t)$.

Step 3: The liquid boundary $\mathcal{D}(t+dt)$ at time $t+dt$ is obtained by moving between times t and $t+dt$ each surfaces S_m by exploiting the relation (6) and each solid surface Σ_n at the velocity $U^{(n)}(t)\mathbf{e}_3$.

One should note that for such a procedure the following issues are of the utmost importance:

(i) To accurately compute the local average curvature $(\boldsymbol{\sigma}\cdot\mathbf{n})/2$ on each surface S_m in Step 1.

(ii) To efficiently and accurately solve the Stokes problem (1)-(5) in Step 2.

(iii) To adequately select a time step at in Step 3.

This work introduces a suitable treatment to cope with the previous issue (ii).

3. Advocated method

This section presents a new procedure to appropriately solve the problem (1)-(5).

3.1 Auxiliary Stokes flows for cluster involving at least one solid particle.

As soon as $N \geq 1$, each velocity $U^{(n)}$ occuring in (1)-(5) is unknown. Fortunately, it is possible to determine $U^{(1)}(t), \cdots, U^{(N)}(t)$ prior to obtain the liquid flow $(\mathbf{u}, p)$! The trick consists in introducing, for $n = 1, \cdots N$, auxiliary Stokes flows $(\mathbf{u}^{(n)}, p^{(n)})$ obtained without stress on each S_m and when each solid surface Σ_q is motionless for $q \neq m$ with the surface Σ_n of $\mathcal{P}_q$ which translates at the velocity $\mathbf{e}_3$. In other words, the flow $(\mathbf{u}^{(n)}, p^{(n)})$ with stress tensor $\boldsymbol{\sigma}^{(n)}$ satisfies (1) and the following boundary conditions

$$\mathbf{u}^{(n)} = \delta_{nq}\mathbf{e}_3 \text{ on } \Sigma_q \text{ for } q = 1, \cdots, N \tag{7}$$

$$\boldsymbol{\sigma}^{(n)} \cdot \mathbf{n} = \mathbf{0} \text{ on } S_m \text{ for } m = 0, \cdots, M. \tag{8}$$

In addition, one supplements (1), (7)-(8) with the additionnal conditions

$$\int_{S_m(t)} \mathbf{u}^{(n)} \cdot \mathbf{n}\, dS = 0 \text{ on } S_m \text{ for } m = 0, ..., M. \tag{9}$$

Denoting by $\partial\mathcal{D}$ the liquid boundary, the reciprocal identity [2] for the flows $(\mathbf{u}, p)$ and $(\mathbf{u}^{(n)}, p^{(n)})$ reads

$$\int_{\partial\mathcal{D}} \mathbf{u}^{(n)} \cdot \boldsymbol{\sigma} \cdot \mathbf{n}\, dS = \int_{\partial\mathcal{D}} \mathbf{u} \cdot \boldsymbol{\sigma}^{(n)} \cdot \mathbf{n}\, dS. \tag{10}$$

Enforcing the relations (5) by exploiting the aformentionned identity (10) and the boundary conditions (2)-(3) and (7)-(8), one then arrives at the N-equation linear system

$$\sum_{q\geq 1} \Big(\int_{\Sigma_q} \mathbf{e}_3 \cdot \boldsymbol{\sigma}^{(n)} \cdot \mathbf{n}\, dS \Big) U^{(q)}(t) = (\rho - \rho_n)\mathcal{V}_n\, g$$
$$+ \sum_{m\geq 0} \int_{S_m} \mathbf{u}^{(n)} \cdot (\rho \mathbf{g}\cdot\mathbf{x} - p_m + \gamma_m \boldsymbol{\nabla}_S \cdot \mathbf{n})\, \mathbf{n}\, dS \quad \text{for } n = 1, \cdots, N. \tag{11}$$

Furthemore, the pressure p_m is uniform in the bubble B_m which leads, in conjection with (5), to

$$\sum_{q\geq 1}\Big(\int_{\Sigma_q}\mathbf{e}_3\cdot\boldsymbol{\sigma}^{(n)}\cdot\mathbf{n}\,dS\Big)U^{(q)}(t)=(\rho-\rho_n)\mathcal{V}_n\,g + \sum_{m\geq 0}\int_{S_m}\mathbf{u}^{(n)}\cdot(\rho\mathbf{g}\cdot\mathbf{x}+\gamma_m\boldsymbol{\nabla}_S\cdot\mathbf{n})\,\mathbf{n}\,dS \quad \text{for } n=1,\cdots,N. \tag{12}$$

It is possible (and here admitted) to prove, invoking the energy dissipation in Stokes flow, that (12) is well-posed (i. e. presents a non-singular matrix). Note that, one solely needs to evaluate the surface quantities $\mathbf{u}^{(n)}$ on each S_m and $\boldsymbol{\sigma}^{(n)}\cdot\mathbf{n}$ on each Σ_q to obtain the translational velocity $U^{(q)}(t)\mathbf{e}_3$ of the particle $\mathcal{P}_q$. As shown in the next subsection, those required key surface quantities $\mathbf{u}^{(n)}$ and $\boldsymbol{\sigma}^{(n)}\cdot\mathbf{n}$ are calculated by inverting relevant boundary-integral equations on the entire liquid boundary $\partial\mathcal{D}$.

3.2 Relevant boundary-integral equations

3.2.1 Three-dimensionnal formulation

For a Stokes flow $(\mathbf{u},p)$ with stress tensor $\boldsymbol{\sigma}$ obeying (1) with prescribed values of the stress $\boldsymbol{\sigma}\cdot\mathbf{n}$ on each S_m and of the velocity $\mathbf{u}$ on each Σ_n, one has the key coupled *regularized* boundary-integral equations (see for instance [5]),

$$-8\mu\pi\mathbf{u}(\mathbf{x}_0)+\sum_{m\geq 0}\int_{S_m}\mu[\mathbf{u}(\mathbf{x})-\mathbf{u}(\mathbf{x}_0)]\cdot\mathbf{T}(\mathbf{x},\mathbf{x}_0)\cdot\mathbf{n}(\mathbf{x})dS-\sum_{n\geq 1}\int_{\Sigma_n}\mathbf{G}(\mathbf{x},\mathbf{x}_0)\cdot\boldsymbol{\sigma}\cdot\mathbf{n}(\mathbf{x})dS = \sum_{m\geq 0}\int_{S_m}\mathbf{G}(\mathbf{x},\mathbf{x}_0)\cdot\boldsymbol{\sigma}\cdot\mathbf{n}(\mathbf{x})dS \qquad \text{for } \mathbf{x}_0 \text{ on } S_m \tag{13}$$

and

$$\sum_{m\geq 0}\int_{S_m}\mu[\mathbf{u}(\mathbf{x})-\mathbf{u}(\mathbf{x}_0)]\cdot\mathbf{T}(\mathbf{x},\mathbf{x}_0)\cdot\mathbf{n}(\mathbf{x})dS-\sum_{n\geq 1}\int_{\Sigma_n}\mathbf{G}(\mathbf{x},\mathbf{x}_0)\cdot\boldsymbol{\sigma}\cdot\mathbf{n}(\mathbf{x})dS = +8\mu\pi\mathbf{u}(\mathbf{x}_0)+\sum_{m\geq 0}\int_{S_m}\mathbf{G}(\mathbf{x},\mathbf{x}_0)\cdot\boldsymbol{\sigma}\cdot\mathbf{n}(\mathbf{x})dS \qquad \text{for } \mathbf{x}_0 \text{ on } \Sigma_n \tag{14}$$

where the second-rank tensor $\mathbf{G}$ and third-rank stress tensor $\mathbf{T}$ are defined as [3]

$$G(\mathbf{x},\mathbf{x}_0)=\frac{\mathbf{I}}{|\mathbf{x}-\mathbf{x}_0|}+\frac{(\mathbf{x}-\mathbf{x}_0)\otimes(\mathbf{x}-\mathbf{x}_0)}{|\mathbf{x}-\mathbf{x}_0|^3}; \tag{15}$$

$$T(\mathbf{x},\mathbf{x}_0)=-6\,\frac{(\mathbf{x}-\mathbf{x}_0)\otimes(\mathbf{x}-\mathbf{x}_0)\otimes(\mathbf{x}-\mathbf{x}_0)}{|\mathbf{x}-\mathbf{x}_0|^5.} \tag{16}$$

with $\mathbf{I}$ the identity tensor. Clearly, solving (13)-(14) permits one to get the unknown vectors $\mathbf{u}$ on S_m and $\boldsymbol{\sigma}\cdot\mathbf{n}$ on Σ_n from the knowledge of $\mathbf{u}$ on Σ_n and $\boldsymbol{\sigma}\cdot\mathbf{n}$ on S_m.

3.2.2 Axisymmetric formulation

Since we restrict the analysis to the axisymmetric configuration depicted in Fig.1, we adopt cylindrical coordinates (r,ϕ,z) with $r=\sqrt{x^2+y^2}$, $z=x_3$ and ϕ the azimuthal angle in the range $[0,2\pi]$. We set $\mathbf{u}=u_r\mathbf{e}_r+u_z\mathbf{e}_z=u_\alpha\mathbf{e}_\alpha$ (with $\alpha=r,z$), $\mathbf{f}=\boldsymbol{\sigma}\cdot\mathbf{n}=f_r\mathbf{e}_r+f_z\mathbf{e}_z=f_\alpha\mathbf{e}_\alpha$ and $\mathbf{n}=n_r\mathbf{e}+n_z\mathbf{e}_z=n_\alpha\mathbf{e}_\alpha$ and introduce the traces $\mathcal{L}_n$ of Σ_n and $\mathcal{L}_m$ of S_m in the $\phi=0$ half plane.

Integrating over ϕ the equations (13)-(14), then yields the equivalent coupled boundary equations

$$-8\pi u_\alpha(\mathbf{x}_0) + \sum_{m\geq 0}\int_{\mathcal{L}_m} \mu[u_\beta(\mathbf{x}) - u_\beta(\mathbf{x}_0)]\, C_{\alpha\beta}(\mathbf{x},\mathbf{x}_0)dl - \sum_{n\geq 1}\int_{\mathcal{L}_n} B_{\alpha\beta}(\mathbf{x},\mathbf{x}_0) f_\beta n_\beta(\mathbf{x})dl$$
$$= \sum_{m\geq 0}\int_{\mathcal{L}_m} B_{\alpha\beta}(\mathbf{x},\mathbf{x}_0) f_\beta n_\beta(\mathbf{x})dl \quad \text{for } \mathbf{x}_0 \text{ on } \mathcal{L}_m \tag{17}$$

and

$$\sum_{m\geq 0}\int_{\mathcal{L}_\Updownarrow} \mu[u_\beta(\mathbf{x}) - u_\beta(\mathbf{x}_0)] C_{\alpha\beta}(\mathbf{x},\mathbf{x}_0)dl - \sum_{n\geq 1}\int_{\mathcal{L}_n} B_{\alpha\beta}(\mathbf{x},\mathbf{x}_0) f_\beta n_\beta(\mathbf{x})dl$$
$$= 8\pi u_\alpha(\mathbf{x}_0) + \sum_{m\geq 0}\int_{\mathcal{L}_m} B_{\alpha\beta}(\mathbf{x},\mathbf{x}_0) f_\beta n_\beta(\mathbf{x})dl \quad \text{for } \mathbf{x}_0 \text{ on } \mathcal{L}_n \tag{18}$$

for $\alpha = r, z$, the differential arc length dl in the $\phi = 0$ plane and the so-called single-layer and double-layer 2×2 square matrices $B_{\alpha\beta}(\mathbf{x},\mathbf{x}_0)$ and $C_{\alpha\beta}(\mathbf{x},\mathbf{x}_0)$ given in Pozrikidis [5]. Note that a summation over $\beta = r, z$ holds in (17)-(18).

3.2.3 Resulting boundary-integral equations for the axisymmetric Stokes flow problem

Dealing with our axisymmetric problem (1)-(4), we first evaluate for each axisymmetric flow $(\mathbf{u}^{(n)}, p^{(n)})$ the needed vectors $\mathbf{u}^{(n)} = u_\alpha^{(n)}\mathbf{e}_\alpha$ on each S_m and $\boldsymbol{\sigma}^{(n)} = f_\beta^{(n)}\mathbf{e}_\beta$ on each Σ_q. We perform this calculation by inverting (17)-(18) for $u_z^{(n)} = \delta_{nq}$ and $u_r^{(n)} = 0$ on each Σ_q and $\boldsymbol{\sigma}^{(n)}\cdot\mathbf{n} = 0$ on each S_m. Once both the velocity and stress vectors are known on each surfaces Σ_q and S_m, one then obtains each velocity $U^{(q)}(t)$ by solving the linear system (12).

Finally, we gain the required velocity $\mathbf{u} = u_\alpha\mathbf{e}_\alpha$ on each S_m by inverting one more time (17)-(18) using the boundary conditions (2)-(3), i. e.

$$-8\pi u_\alpha(\mathbf{x}_0) + \sum_{m\geq 0}\int_{\mathcal{L}_m} \mu[u_\beta(\mathbf{x}) - u_\beta(\mathbf{x}_0)]\, C_{\alpha\beta}(\mathbf{x},\mathbf{x}_0)dl - \sum_{n\geq 1}\int_{\mathcal{L}_n} B_{\alpha\beta}(\mathbf{x},\mathbf{x}_0) f_\beta n_\beta(\mathbf{x})dl$$
$$= \sum_{m\geq 0}\int_{\mathcal{L}_m} B_{\alpha\beta}(\mathbf{x},\mathbf{x}_0)[\rho\mathbf{g}\cdot\mathbf{x} + \gamma_m\boldsymbol{\nabla}_S\cdot\mathbf{n}]\, n_\beta(\mathbf{x})dl \quad \text{for } \mathbf{x}_0 \text{ on } \mathcal{L}_m \tag{19}$$

and

$$\sum_{m\geq 0}\int_{\mathcal{L}_m} \mu[u_\beta(\mathbf{x}) - u_\beta(\mathbf{x}_0)] C_{\alpha\beta}(\mathbf{x},\mathbf{x}_0)dl - \sum_{n\geq 1}\int_{\mathcal{L}_n} B_{\alpha\beta}(\mathbf{x},\mathbf{x}_0) f_\beta n_\beta(\mathbf{x})dl = +8\pi U^{(n)}(t)\mathbf{e}_3(\mathbf{x}_0)$$
$$+ \sum_{m\geq 0}\int_{\mathcal{L}_m} B_{\alpha\beta}(\mathbf{x},\mathbf{x}_0)[\rho\mathbf{g}\cdot\mathbf{x} + \gamma_m\boldsymbol{\nabla}_S\cdot\mathbf{n}]\, n_\beta(\mathbf{x})dl \quad \text{for } \mathbf{x}_0 \text{ on } \mathcal{L}_n \tag{20}$$

for $\alpha = r, z$ and γ_m uniform on each surface S_m. In summary, our approach consists, for $N \geq 1$ solid particle(s), in inverting $N+1$ boundary-integral equations (17)-(18).

4. Numerical method

The coupled boundary-integral equation (17)-(18) are numerically inverted by appealing to the following key steps (see for further details [4, 1]):

(i) First, the entire contour $\mathcal{L} = \mathcal{L}_n \cup \mathcal{L}_n$ is divided into N_e curved boundary elements with the $\mathcal{L}_0$ truncated free surface. Each boundary element has N_c collocation points spread with a uniform distribution. An isoparametric approximation is used for the components $\mathbf{u}$ and $\mathbf{f} = \boldsymbol{\sigma}\cdot\mathbf{n}$ on each boundary element.

For the nodes located on $\mathcal{L}_m$, the vectors $\mathbf{U}$ and $\mathbf{F_d}$ collect the unknown and prescribed components of $\mathbf{u}$ and $\mathbf{f}$. In a similar fashion, $\mathbf{F}$ and $\mathbf{U_d}$ are the vectors associated with the unknown and given values of $\mathbf{f}$ and $\mathbf{u}$ at the nodes of the solid contours $\mathcal{L}_n$. Finally, once the coupled boundary-integral equations (17)-(18) are discretized, these vectors satisfy indeed the $2N_eN_c$-equation linear system

$$\mathbf{U} + \mathbf{C} \cdot \mathbf{U} - \mathbf{B_1} \cdot \mathbf{F} = -\mathbf{B_2} \cdot \mathbf{F_d} \quad \text{for } \mathbf{x}_0 \text{ on } \cup_{m\geq 0}\mathcal{L}_m, \tag{21}$$

$$\mathbf{C} \cdot \mathbf{U} - \mathbf{B_1} \cdot \mathbf{F} = -\mathbf{U_d} + \mathbf{B_2} \cdot \mathbf{F_d} \quad \text{for } \mathbf{x}_0 \text{ on } \cup_{n\geq 1}\mathcal{L}_n. \tag{22}$$

The matrices $\mathbf{B_1}$, $\mathbf{B_2}$ and $\mathbf{C}$ involve integrations of the quantities $B_{\alpha\beta}$ and $C_{\alpha\beta}$ introduced in §3.2.2 over the entire contours $\cup_{m\geq 0}\mathcal{L}_m$ and $\cup_{n\geq 1}\mathcal{L}_n$. .

(ii) One finds the solution (**U,F**) of (21)-(22) by Gaussian elimination.

(iii) The shape of each surface S_m and the position of each Σ_n if $N \geq 1$ is tracked in time using the boundary condition (6) and solving the equation $d\mathbf{x}/dt = \mathbf{u}(\mathbf{x}, t)$ for each nodal point. A Runge-Kutta-Fehlberg method performs this task using a time-step selected by controlling the errors for the second and third-order schemes. Furthermore, as the distance between two surfaces tends to zero, the adjusted time step is then very small and the computations is stopped.

5. Conclusions

Preliminary numerical results will be exposed at the oral presentation for a cluster made of one bubble and one spherical solid particle. Furthermore, this particular case will be dicussed and compared with the two-bubbles configurations studied in [4, 1]

References

[1] M. Guémas, F. Pigeonneau, and A. Sellier. Gravity-driven migration of one bubble near a free surface: surface tension effects. In M. H. Aliabadi P. Prochazca, editor, *Advances in Boundary Element & Meshless Techniques XIII*, 2012.

[2] J. Happel and H. Brenner. *Low Reynolds number hydrodynamics.* Martinus Nijhoff Publishers, The Hague, 1983.

[3] S. Kim and S. J. Karrila. *Microhydrodynamics. Principles and selected applications.* Butterworth-Heinemann, Boston, 1991.

[4] F. Pigeonneau and A. Sellier. Low-reynolds-number gravity-driven migration and deformation of bubbles near a free surface. *Phys. Fluids*, 23:092302, 2011.

[5] C. Pozrikidis. *Boundary integral and singularity methods for linearized viscous flow.* Cambridge University Press, Cambridge, 1992.